Transverse two-stream instability of a beam with a Bennett profile

David H. Whittum

Stanford Linear Accelerator Center

Stanford University, Stanford CA 94309

(Received)

A relativistic electron beam magnetically self-focused in a plasma is subject to an electrostatic hose instability. A linear theory of hose growth is formulated taking into account nonlinear focusing of the beam and collisionless damping due to a plasma gradient. Theory is compared to particle-in-cell simulations of three-dimensional transport of a beam with a Bennett profile, through a broad uniform plasma, as well as a plasma channel matched to the beam.

PACS: 29.27.Bd, 52.35.-g, 41.75Ht, 52.65.+z

I. INTRODUCTION

The only fundamental barrier to a compact TeV-energy plasma-based accelerator is transverse stability. Since the pioneering work of Bennett,[1] Budker[2], Fainberg, and others[3] considerable theoretical[4,5] and experimental work[6,7,8] has shown that plasmas provide strong coupling, for focusing and for acceleration making use of relativistic electron beams. At the same time this strong coupling extends to strong *deflection* and *break-up* of the beam, and this has motivated vigorous efforts over many years to understand transverse instabilities of the self-focused equilibrium.[9] This work has concentrated on the resistive hose instability,[10,11,12] and the filamentation instability,[13,14] with scant reference to the transverse two-stream instability.[15] To-date there has been no analytic treatment of the transverse electron-coupled effect for the (non-laminar) magnetically self-focused beam in cylindrical geometry and a recent study by Krall and Joyce[16] suggests that this would be quite useful to have. Furthermore, results for the ion-focused regime[17,18] and for a slab geometry[19] suggest that the electrostatic mode of beam break-up may be more severe than any other, in the limit of large skin-depth and this motivates the present analysis.

In Sec. II linear theory is formulated for an arbitrary matched relativistic beam, and an arbitrary cold continuous plasma geometry with collisionless skin-depth large compared to the beam. The resulting system is reduced to a macroparticle model described in terms of a distribution in betatron tune determined by the beam ("distributed mass model"), and a transverse impedance which is

determined from the spatial beam and plasma profiles. We specialize to the case of a beam with a Bennett profile,[1] adopting the tune distribution of Lee.[10] The variety of possible plasma profiles (and the effect of gradient-induced damping) is sampled by considering two extremes: a broad plasma (Sec. III) and a narrow plasma channel matched to the beam (Sec. IV). For each case, asymptotic growth is computed, compared to the results of linear simulations, and particle-in-cell simulations.

II. LINEAR FORMULATION

We consider a relativistic electron beam with equilibrium density $n_{b,}$ a function of the radial coordinate r and the beam coordinate $\tau \sim t - z/c$, where t is time, z is axial displacement and c is the speed of light. The beam propagates in the z-direction through a smooth plasma of density $n_e >> n_b$, maintaining quasineutrality in equilibrium, provided $\omega_e \tau_r >> 1$ where τ_r is the beam current rise time and ω_e is the angular plasma frequency, $\omega_e^2 = 4\pi n_e e^2/m$, with m the electron mass and $-e$ the electron charge. Negligible plasma return current flows through the beam volume in the limit of large plasma skin-depth $c/\omega_e >> a$, with a the Bennett waist. Ion-motion and radiative effects are neglected. The equilibrium plasma is assumed stationary in τ, either preformed, or created rapidly by the beam head.[4]

A. Rigid Beam

To the Bennett equilibrium we consider first a *rigid* beam displacement, $\vec{Y} = Y\hat{y}$ in the *y*-direction, as depicted in Fig. 1. The perturbed beam charge density is $\rho_{b1} = -\vec{\nabla}_\perp \rho_{b0} \bullet \vec{Y}$, with ρ_{b0} the equilibrium charge density and $\vec{\nabla}_\perp$ the gradient in the transverse coordinates. From the Vlasov equation one can show that momentum conservation takes the form

$$\frac{\partial^2 \vec{Y}}{\partial z^2} = -\frac{1}{\gamma Q}\int d^2 r_\perp \left\{ \rho_{b1}\vec{\nabla}_\perp \psi_0 + \rho_{b0}\vec{\nabla}_\perp \psi_1 \right\}, \tag{1}$$

where $Q = \int d^2 r_\perp \rho_{b0}$ is the beam charge per unit length and γ is the Lorentz factor for the beam. Here $\psi = A - \phi$ is the "pinch" potential, with *A* and ϕ the axial vector, and electrostatic potentials in the Lorentz gauge, normalized by e/mc^2 so as to be dimensionless. The subscripts "0" and "1" denote the equilibrium and perturbed components. Combining Maxwell's equations (absent magneto-induction and radiation) and the non-relativistic cold fluid equations for the plasma, one obtains,

$$\vec{\nabla}_\perp \bullet \left(\varepsilon \vec{\nabla}_\perp \tilde{\phi}_1\right) = -\vec{\nabla}_\perp \bullet \left(k_b^2 \tilde{Y}\hat{y}\right), \tag{2}$$

$$\vec{\nabla}_\perp \bullet \left(\vec{\nabla}_\perp \tilde{A}_1\right) = -\vec{\nabla}_\perp \bullet \left(k_b^2 \tilde{Y}\hat{y}\right), \tag{3}$$

where the cold-plasma dielectric function is

$$\varepsilon = 1 + \frac{\omega_e^2(r)}{p(p+\nu)}, \tag{4}$$

and a Laplace transform (denoted by the overtilde) has been made in τ, with p the Laplace transform variable. The quantity $k_b^2(r)=4\pi n_b e^2/mc^2$. The collision rate ν is assumed constant. The solution to Eq. (2) may be decomposed as

$$\tilde{\phi_1}(r,\theta,z,p) = \hat{\phi}(r,p)\tilde{Y}(z,p)\sin\theta, \tag{5}$$

with θ the polar angle in the transverse plane. The function $\hat{\phi}$ is determined once the plasma and beam profiles are specified, from

$$\frac{1}{r}\frac{\partial}{\partial r}r\left(\varepsilon\frac{\partial\hat{\phi}}{\partial r}-\frac{\hat{\phi}}{r^2}\right)=-\frac{\partial k_b^2}{\partial r}. \tag{6}$$

Given $\hat{\phi}$, the solution for ψ_1 may be obtained as

$$\tilde{\psi}_1(r,\theta,z,p) = \hat{\psi}(r,p)\tilde{Y}(z,p)\sin\theta, \tag{7}$$

where

$$\hat{\psi}(r,p) = \hat{\phi}(r,\infty) - \hat{\phi}(r,p). \tag{8}$$

Combining Eqs. (1) and (7) there results

$$\frac{\partial^2\tilde{Y}}{\partial z^2}+k_s^2\tilde{Y}=k_s^2 Z(p)\tilde{Y}, \tag{9}$$

where the slosh wavenumber k_s depends only on the beam profile,

$$k_s^2 = -\frac{4\pi^2 e}{mc^2 \gamma Q}\int dr\, r\, \rho_{b0}^2 , \qquad (10)$$

and is just $k_s/k_\beta = 3^{-1/2}$ for the Bennett equilibrium, $n_b(r) = n_b(0)/(1+r^2/a^2)^2$, with $k_\beta = k_b(0)/(2\gamma)^{1/2}$ the wavenumber for small amplitude betatron oscillations.

The normalized transverse impedance Z is given by

$$k_s^2 Z(p) = -\frac{\pi}{\gamma Q}\int dr\, \rho_{b0}\frac{\partial}{\partial r}(r\hat{\psi}) , \qquad (11)$$

and depends on both the beam and plasma profiles. In general $Z(0) = 1$ and Z vanishes at large p, confirming that a slowly varying beam displacement is easily neutralized by the plasma and is not guided, while a suddenly offset centroid is attracted to the center axis.

In the time domain Eq. (9) takes the form

$$\left(\frac{\partial^2}{\partial z^2} + k_s^2\right) Y(z,\tau) = k_s^2 \int_0^\tau d\tau' W(\tau - \tau') Y(z,\tau') , \qquad (12)$$

where the wakefield is given by

$$W(\tau) = \frac{1}{2\pi i}\int_{-i\infty+0^+}^{+i\infty+0^+} dp\, e^{p\tau} Z(p) . \qquad (13)$$

B. Distributed Tune Model

From Eq. (9) or Eq. (12) one can in principle compute analytically the asymptotic growth, or numerically the detailed

evolution of the beam centroid. However this formulation applies to a rigid displacement, and is limited to a short range, $k_\beta z \sim O(1)$, for over a few betatron periods one expects phase-mixing in beam electron motion to dissipate any coherent sloshing of the centroid.

To quantify this effect we adopt a macroparticle model, following Lee's work on the resistive-hose problem.[10] The beam centroid is represented as an aggregate of macroparticle displacements, $Y = \int d\alpha\, g(\alpha) Y_\alpha$. The "mass distribution" $g=6\alpha(1-\alpha)$ is normalized to unit integral, the dimensionless parameter α lies in the range [0,1], and the components satisfy

$$\frac{\partial^2 \tilde{Y}_\alpha}{\partial z^2} + \alpha k_\beta^2 \tilde{Y}_\alpha = \alpha k_\beta^2 Z(p)\tilde{Y}, \tag{14}$$

or in the time domain,

$$\left(\frac{\partial^2}{\partial z^2} + \alpha k_\beta^2\right) Y_\alpha(z,\tau) = \alpha k_\beta^2 \int_0^\tau d\tau' W(\tau-\tau') \bar{Y}(z,\tau') . \tag{15}$$

The corresponding dispersion relation takes the form $1=(1+\chi)Z$, where the susceptibility

$$\begin{aligned}\chi(\beta) &= \int d\alpha\, g(\alpha) \frac{\beta}{\alpha-\beta} \\ &= 3\beta + 6\beta^2 \left\{(1-\beta) ln\left(\frac{\beta-1}{\beta}\right) - 1\right\},\end{aligned} \tag{16}$$

with $\beta = k^2/k_\beta^2$, and k the axial wavenumber. Inverting Eq. (15), one obtains the solution for the centroid,

$$Y(z,\tau) = -\frac{1}{4\pi^2}\int_{-i\infty+0^+}^{+i\infty+0^+} dp \int_{-\infty-i0^+}^{\infty-i0^+} dk\, \frac{e^{p\tau+ikz}}{pk}\,\frac{\chi}{1-(1+\chi)Z}, \qquad (17)$$

and a unit initial displacement is assumed.

With a saddle point evaluation of this integral one can show that the saturation length L_s, scales according to $k_\beta L_s/\omega_e\tau \sim L$, with amplitude at saturation given by

$$|Y| \approx A(\omega_e\tau)^{-1/2} exp(\Gamma\omega_e\tau), \qquad (18)$$

where henceforth we abbreviate $\omega_e=\omega_e(0)$. The dimensionless parameters L, A and Γ are functions of the normalized collision rate $\tilde{\nu}=\nu/\omega_e$; the functional form depends on the plasma profile, through Z, and the beam equilibrium through Z and g. The form of the algebraic factor in Eq. (18) is specific to a unit initial displacement, and appropriate for $\omega_e\tau>1$.

In the next two sections we apply this formulation to describe hose evolution in two illustrative plasma geometries.

III. BROAD UNIFORM PLASMA

For the uniform plasma, Eq. (6) can be solved in closed form and the impedance is just

$$Z(p) = \frac{\omega_e^2}{\omega_e^2 + p(p+\nu)}. \qquad (19)$$

In the time domain the wake is

$$W(\tau) = \frac{\omega_e^2}{\Omega_e} \sin(\Omega_e \tau) \exp\left(-\frac{\nu\tau}{2}\right), \tag{20}$$

where Ω_e is the oscillation frequency with damping correction, $\Omega_e^2 = \omega_e^2 - \nu^2/4$.[20]

For a short propagation range, phase-mixing is a small effect and the asymptotic form of the centroid may be computed from Eq. (9). The result is identical in form to that derived for the electron-hose instability.[15] For $k_s z << \omega_e \tau$, the amplitude varies as $Y \sim exp(z/L_g)^{2/3}$, where $k_s L_g \sim 0.7(\omega_e \tau)^{-1/2}$. Collisions produce convection, with peak growth at $\nu\tau_{sat} \sim 2.5(k_s z)\tilde{\nu}^{-1/2}$, and peak amplitude varying as $exp(z/L_g)$ where $k_s L_g \sim 2\tilde{\nu}^{1/2}$ and $\tilde{\nu} = \nu/\omega_e$.

For a longer range, phase-mixing is expected to be important, and we make use of the Eq. (15) to describe the linear evolution. The dispersion relation is analytically solvable for the roots p as functions of β parameterized by $\tilde{\nu}$.[16] From the solutions $p(\beta,\tilde{\nu})$, the coefficients L, A and Γ may be extracted. Results are well-fit on the interval $0<\tilde{\nu}<2$, by

$$\Gamma \approx 1.0945 - 0.5137\tilde{\nu} + 0.0783\tilde{\nu}^2, \tag{21}$$

$$A \approx 0.408 + 0.119\tilde{\nu} + 0.027\tilde{\nu}^2, \tag{22}$$

$$L \approx 3.365 + 0.0145\tilde{\nu} - 0.092\tilde{\nu}^2 - 0.037\tilde{\nu}^3, \tag{23}$$

Thus saturation occurs after about $\omega_e\tau$ exponentiations. For a large collision rate growth can be reduced substantially.

To check this model we make comparison with a particle-in-cell (PIC) simulation.[21] This simulation advances the plasma variables (transverse position and nonrelativistic momentum) in the beam coordinate τ, with a leap-frog algorithm governed by the electrostatic potential gradient. The corresponding beam variables are advanced in z by a leap-frog algorithm, governed by the pinch potential gradient. The neutralizing ion background is fixed. This formulation is consistent with (and limited to) large plasma skin-depth, an ultra-relativistic beam, and negligible radiative effects. Further details of the simulation are described in Appendix A.

Results for evolution in $k_\beta z$ for $\omega_e\tau=2\pi$ are depicted in Fig. 2, overlayed with the numerical solution of the linear model, Eq. (15). The saturation amplitude from the PIC simulation is shown in Fig. 3, overlayed with the model results, which are evidently quite adequate. A least-squares fit to the PIC result for $\omega_e\tau<15$ gives $A_0\sim0.5$, $\Gamma_0\sim1.0$, in fair agreement with theory.

IV. GRADED PLASMA

To illustrate the effect of a plasma gradient we consider a plasma profile matched to the beam. In this case computation of the impedance is a bit more involved than for a uniform plasma. For a short pulse the simplest approximation would take over Eq. (12), directly. In general, to obtain the exact result we must solve Eq. (6) numerically for a collection of real frequencies ω_j, and corresponding

complex $p_j=-i\omega_j+\eta$, with $\eta<<\omega_e$ real and positive. In this way the impedance $Z_j=Z(p_j)$ may be computed using Eqs. (8) and (11). The wake is then determined with a discrete Fourier transform, as described in Appendix B. The result for the impedance Z for $\nu=0$ is depicted in Fig.4, with the corresponding wake in Fig. 5. This result is roughly fit with a single-mode Lorentzian as in Eq. (20), with resonant frequency $\omega_L=0.71\omega_e$, damping rate $\nu_L=0.34\omega_e$ and frequency with damping correction $\Omega_L=0.69\omega_e$. This fit is overlayed in Fig. 5. Thus to a fair approximation the effect of the plasma gradient is collisonless damping with a low $Q=\omega_L/\nu_L\sim 2$.

Having fit the impedance with a Lorentzian, Eqs. (21)-(23) immediately provide the parameters determining the asymptotic growth in Eq. (18): $\Gamma\sim 0.86$, $A\sim 0.47$ and $L\sim 3.4$ (it being understood that in applying these in Eq. (18) ω_e should be replaced by ω_L.)

To check this result we return to the PIC simulation. Results for evolution in $k_\beta z$ for $\omega_e\tau=2\pi$ are depicted in Fig. 6, overlayed with the numerical solution of the model, Eq. (15), in the time-domain. The saturation amplitude from the PIC simulation is shown in Fig. 7, overlayed with the model results, which are evidently adequate. A least-squares fit to the PIC result gives $A\sim 0.4$, $\Gamma\sim 0.97$. It should be note for this case that the numerical plasma and beam profiles are cut-off at about twice the Bennett radius. This results in a small ringing component in the numerical wake which tends to exaggerate growth slightly.

V. CONCLUSIONS

Small amplitude evolution of the transverse two-stream instability has been formulated in terms of Lee's "mass" distribution for the Bennett beam, with the cold-plasma response summarized in terms of an impedance. The character of this impedance and its effect on growth has been examined for two illustrative cases, a uniform plasma, and a graded Bennett plasma. We found that hose growth in a uniform plasma is quite rapid, saturating only after of order $\omega_e\tau$ exponentiations in the collisionless case. For the graded plasma the saturation exponent is smaller, but still large enough to cause concern for long range propagation.

In sum, we have produced some simple scalings and a macroparticle model that permits study of such phenomena short of PIC simulation.

To put this work in perspective note that previous analyses of transverse stability have been performed in the limit of short plasma skin-depth where the effect of plasma return current is pervasive. Often also the plasma was assumed highly collisional, due to a low ionization fraction. In this limit, resistive hose growth has been a serious concern, with growth length scaling as $k_sL_g\sim\Gamma/\tau$, and Γ the diffusion time-scale. On the other hand, in the different limit, of large collisionless skin-depth and modest collision rate, $\omega_e\Gamma\sim\omega_e/\nu>>1$ and the resistive hose instability is benign in comparison to the electrostatic hose. Moreover filamentation is known to be negligible for large skin-depth.[12,13] Thus for propagation of fine, high-energy

beams in plasma the transverse two-stream instability is the more serious concern.

These results also point toward some possible solutions. Firstly, these features of beam break-up as they would apply to a high-current, broad drive beam could be ameliorated by further modifications of the plasma geometry. (Only the simplest modification was considered here, a monotone gradient.) Secondly, such modifications need not destroy the longitudinal wakefield on-axis, the wakefield of interest for acceleration of a fine "witness" beam. This is because, as we have seen the *effective* transverse impedance involves a convolution with the beam profile, and it is this convolution that lowers the Q of the beam break-up mode. In addition, a *fine* witness bunch (trailing such a *broad* high-current beam) could be controlled to some degree if the bunch is short compared to a plasma period or if the plasma focusing strength is weak compared to the external focusing experienced by the witness bunch.

ACKNOWLEDGMENTS

This work has benefited from discussions with Jonathan Krall and collaboration on related topics with Martin Lampe and Glenn Joyce.

APPENDIX A: PARTICLE-IN CELL SIMULATION

The PIC simulation divides the beam into N_τ ~30 x ($\omega_e\tau/2\pi$) slices and each beam slice is modelled by N~4096-16384 macroparticles. Each slice is initialized at z=0 with a Bennett distribution making use of symmetrized Hammersley deviates along the lines of previous work.[17] The beam particle motion in transverse position $\vec{r}_\perp$ and momentum $\vec{p}_\perp$ (normalized by mc) is governed by the pinch gradient

$$\frac{d\vec{r}_\perp}{dz} = \frac{\vec{p}_\perp}{p_z},$$
$$\frac{d\vec{p}_\perp}{dz} = -\vec{\nabla}_\perp \psi,$$

and these equations are advanced in z with a leap-frog algorithm,[18] with p_z constant, and no slippage in τ.

As for the plasma electrons, one "slice" of M~4096-65536 plasma macroparticles is initialized for each step in z, and passed through the beam from the head to the tail. The plasma initialization loads $M/2$ pairs (x,y) uniformly within the unit circle, by rejection, and quiets the loading by reflection through the origin.[18] This loading subsequently can be deformed to a cut-off Bennett profile. Plasma particle momenta were initialized to zero. The plasma advance is a leap-frog in the beam coordinate τ, governed solely by the electrostatic potential,

$$\frac{d\vec{r}_\perp}{d\tau} = \vec{p}_\perp ,$$
$$\frac{d\vec{p}_\perp}{d\tau} = \vec{\nabla}_\perp \phi ,$$

The initial quasineutral equilibrium is achieved by adiabatic relaxation of the initially uniform plasma in the potential of an undisplaced beam. Typical beam displacements are 10^{-5}-10^{-4} beam radii, small enough to observe saturation prior to strong nonlinearity, and large enough to avoid problems with round-off error.

The potentials are determined from the reduced Maxwell's equations,

$$\nabla_\perp^2 \phi = -\frac{4\pi e}{m c^2}\left(\rho_b + \rho_e + \rho_i\right) ,$$
$$\nabla_\perp^2 A = -\frac{4\pi e}{m c^2}\rho_b .$$

Charge allocation and field interpolation is performed by area-weighting in x-y. These are solved by a fast Fourier transform in x, with periodic boundary conditions, and a finite difference solution in y, with open boundary conditions. Sensitivity to these somewhat artificial boundary conditions was gauged by varying the size of the mesh, and by comparison with three other choices of boundary conditions: periodic in x and y, conducting in x and y, conducting in x and open in y. For the ranges considered here and boundaries displaced by 10-20 beam radii there was no remarkable difference in centroid evolution.

APPENDIX B: EVALUATION OF THE GRADED-PLASMA WAKEFIELD

To compute the wakefield $W(\tau)$ in the case of the graded plasma, we first select a set of $N=2^L$ real equally-spaced times $\tau_k=k\Delta\tau$, $k=0,1,...,N-1$ at which to compute the wake. Typically L~10-14, with 30 points per plasma period. We select frequencies $\omega_j=-\Omega+j\Delta\omega$ where $j=0,1,...,N-1$, $\Delta\omega\Delta\tau=2\pi/N$, and $\Omega=(N-1)\Delta\omega/2$. We then evaluate, as described below, the impedance $Z(p)$ on the corresponding complex $p_j=-i\omega_j+\eta$, with $\eta<<\omega_e$ real and positive; typically η~5x10$^{-3}\omega_e$. Finally we express Eq. (14) in discrete form as

$$W_k = \frac{\Delta\omega}{2\pi i} exp\left(\left[-i\Omega+\eta\right]\tau_k\right)\sum_{j=0}^{N-1} Z_j exp\left(-i\frac{2\pi kj}{N}\right),$$

making use of a fast Fourier transform[22] to evaluate the sum on the right.

Evaluation of the impedance Z_j requires the solution of Eq. (6) which is not analytically tractable in general. Accordingly we difference Eq. (6) on a uniform radial grid $r_j=j\Delta r$, with $j=0,1,2,...M$. The finite difference form used is[18]

$$-\left(\frac{\partial k_b^2}{\partial r}\right)_j \Delta r_j^2 = (r\varepsilon)_{j+1/2}\frac{\hat{\phi}_{j+1}-\hat{\phi}_j}{\Delta r} - (r\varepsilon)_{j-1/2}\frac{\hat{\phi}_j-\hat{\phi}_{j-1}}{\Delta r} - \frac{\Delta r}{r_j}\hat{\phi}_j,$$

where $\Delta r_j^2 = r_{j+1/2}^2 - r_{j-1/2}^2$. The impedance can be expressed as $Z(p)=Z'(p)-Z'(\infty)$, where Z' is computed as an integral

$$\hat{Z} = -\frac{1}{\gamma k_s^2 k_b^2(0)} \int dr\, k_b^2(r) \frac{\partial}{\partial r}(r\hat{\phi}),$$

which can be expressed in terms of a sum

$$\int dr\, k_b^2(r) \frac{\partial}{\partial r}(r\hat{\phi}) \rightarrow \sum_j \left(k_b^2\right)_{j+1/2} \left(r_{j+1}\hat{\phi}_{j+1} - r_j \hat{\phi}_j\right) w_j,$$

where w_0=1/2, w_{M-1}=1/2 and the other w_j=1.

[1]W. H. Bennett, Phys. Rev. **45**, 890 (1934); **98**, 1584 (1955).

[2] G. I. Budker, *Proceedings of the CERN Symposium on High Energy Accelerators and Pion Physics*, (CERN Service d'Information, Geneva, 1956) pp. 68-75; Ya B. Fainberg, *ibid.*, pp. 84-90.

[3] J. D. Lawson, Part. Accel. **3**, 21, (1972); A. A. Kolomensky, *ibid.*, **5**, 7 3 (1973); Ya. B. Fainberg, *ibid.*, **6**, 95 (1975); *Collective Methods of Acceleration*, edited by N. Rostoker and M. Reiser, (Harwood Academic, Amsterdam, 1979).

[4] P. Chen, Phys. Rev. A **45**, 3398 (1992), and references therein.

[5] P. Chen, J. M. Dawson, R. W Huff, and T. Katsouleas, Phys. Rev. Lett. **54**, 693 (1985).

[6] Such work is summarized in S. B. Swanekamp, J. P. Holloway, T. Kammash, and R. M. Gilgenbach, Phys. Fluids B **4**, 1332 (1992).

[7] J. B. Rosenzweig, P. Schoessow, B. Cole, C. Ho, W. Gai, R. Konecny, S. Mtingwa, J. Norem, M. Rosing, and J. Simpson, Phys. Fluids B **2**, 1376 (1990).

[8] H. Nakanishi, Y. Yoshida, T. Ueda, T. Kozawa, H. Shibata, K. Nakajima, T. Kurihara, N. Yugami, Y. Nishida, T. Kobayashi, A. Enomoto, T. Oogoe, H. Kobayashi, B. S. Newberger, S. Tagawa, K. Miya, and A. Ogata, Phys. Rev. Lett **66**, 1870 (1991).

[9]Longitudinal instabilities have been treated extensively (see e.g. H. S. Uhm, J. Appl. Phys. **56**, 2041 (1984)) but are of less concern for highly relativistic beams for which the longitudinal inertia is large.

[10] E. P. Lee, Phys. Fluids **21**, 1327 (1978).

[11] E. J. Lauer, R. J. Briggs, T. J. Fessenden, R. E. Hester, and E. P .Lee, Phys. Fluids **21**, 1344 (1978).

[12] M. Lampe, W. M. Sharp, R. F. Hubbard, E. P. Lee, and R. J. Briggs, Phys. Fluids **27**, 2921 (1984).

[13] E. S. Weibel, Phys. Rev. Lett **2**, 83 (1959); Ronald C. Davidson, *Physics of Nonneutral Plasmas* (Addison-Wesley, Redwood City, 1990).

[14] R. Keinigs and M. E. Jones Phys. Fluids **30**, 252 (1987); J. J. Su, *et al.*, IEEE Trans Plasma Sci., **PS-15**, 192 (1987).

[15] J. D. Lawson, *The Physics of Charged-Particle Beams*, (Clarendon Press, Oxford, 1977).

[16] J. Krall, K. Nguyen, and G. Joyce, Phys. Fluids B **1**, 2099 (1989).

[17] D. R. Welch and T. P. Hughes, Phys. Fluids **B 5**, 339 (1993).

[18] M. Lampe, G. Joyce, S. P. Slinker, and D. H. Whittum, Phys. Fluids **B 5**, 1888 (1993).

[19] D. H. Whittum, Phys. Fluids B **5**, 4432 (1993).

[20]Neglected here is the decoherence in the plasma response resulting from the beam-induced gradient; for a beam sufficiently weak that $n_b/n_e << 2/\omega_e\tau$ this effect is negligible.

[21]Charles K. Birdsall and A. Bruce Langdon, *Plasma Physics Via Computer Simulation*, (MacGraw-Hill, New York, 1985).

[22] W. H. Press, B. P. Flannery, S. A. Teukolsky, and W. T. Vetterling, *Numerical Recipes*, (Cambridge University Press, New York, 1989).

FIG. 1. The transverse two-stream instability of a magnetically self-focused beam proceeds by the electrostatic coupling of hose-like displacements of the beam centroid to hose-like displacements of the plasma electrons.

FIG. 2. Long-range evolution of the beam centroid, normalized by the initial offset in a uniform plasma, from the PIC simulation and the model of Eq. (15) at $\omega_e \tau = 2\pi$.

FIG. 3. Results for saturation amplitude versus pulse length τ normalized by the angular plasma frequency ω_e, in a uniform plasma, from the PIC simulation, the macroparticle model of Eq. (15), and the analytic saddle-point result, Eq. (18). Large amplitude oscillations at later τ result in nonlinear saturation and divergence from the result of linear theory.

FIG. 4. Real and imaginary parts of the transverse impedance Z "seen" by a Bennett beam in a matched Bennett-profile collisionless plasma, obtained from Eqs. (6) and (11).

FIG. 5. The wake corresponding to the impedance of Fig. 4, overlayed with the corresponding fit by a single mode wake.

FIG. 6. Evolution of the beam centroid in a graded plasma, from the PIC simulation and the macroparticle model of Eq. (15) at $\omega_e \tau = 2\pi$.

FIG. 7. Results for saturation amplitude in a graded plasma from the the PIC simulation, the macroparticle model of Eq. (15), and the analytic saddle-point result, Eq. (18).

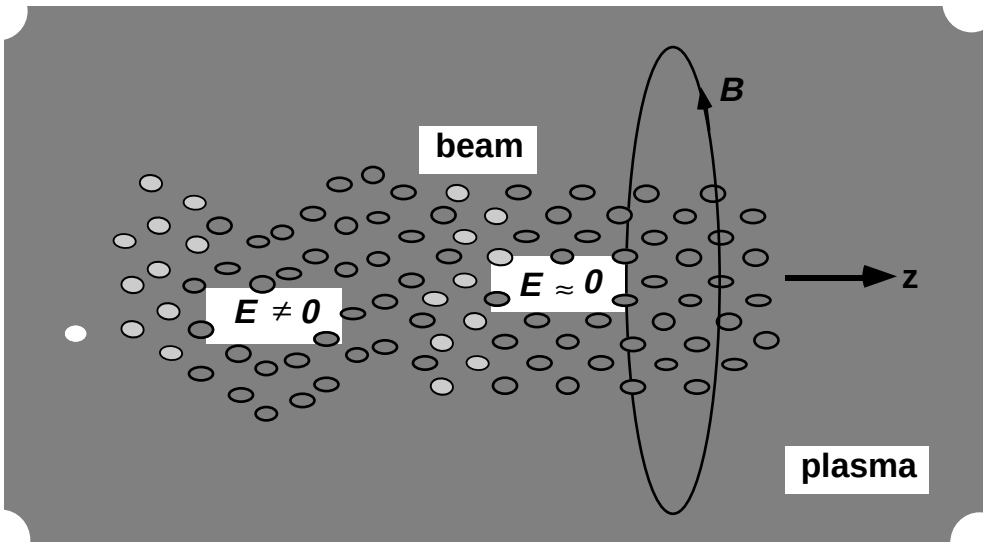

FIG. 1

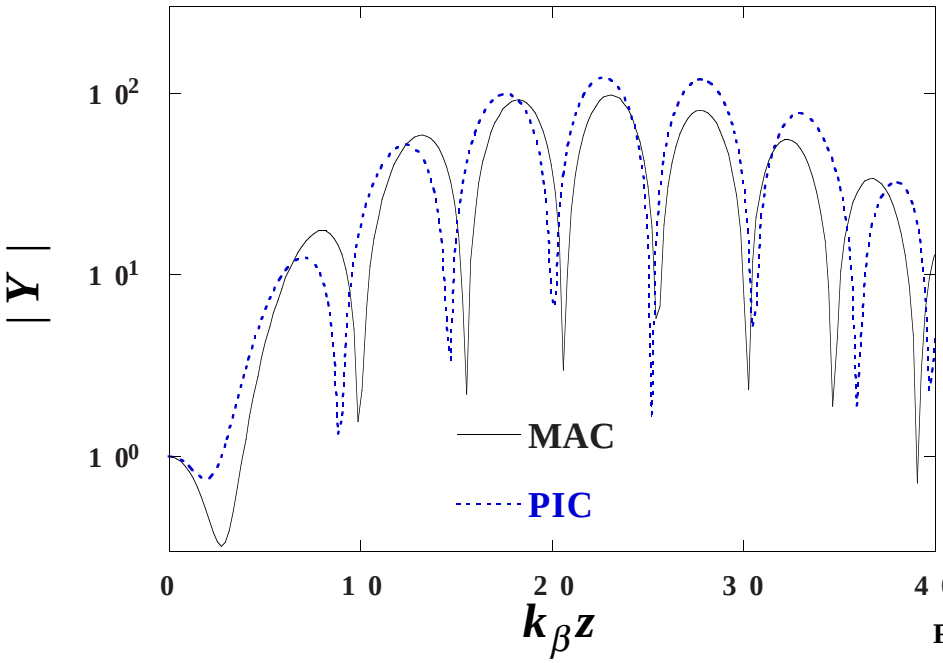

FIG. 2

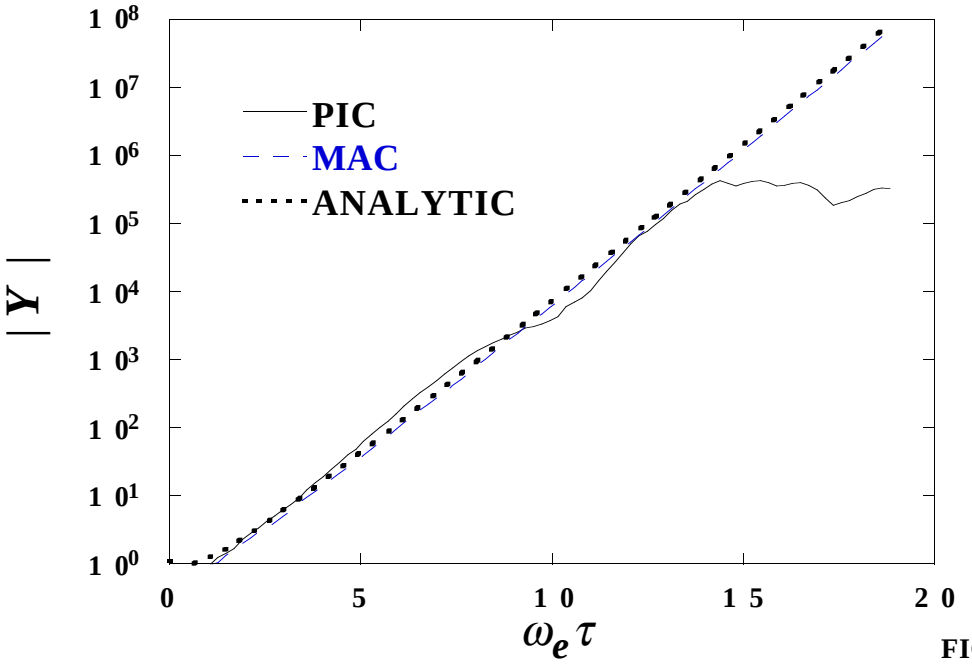

FIG. 3

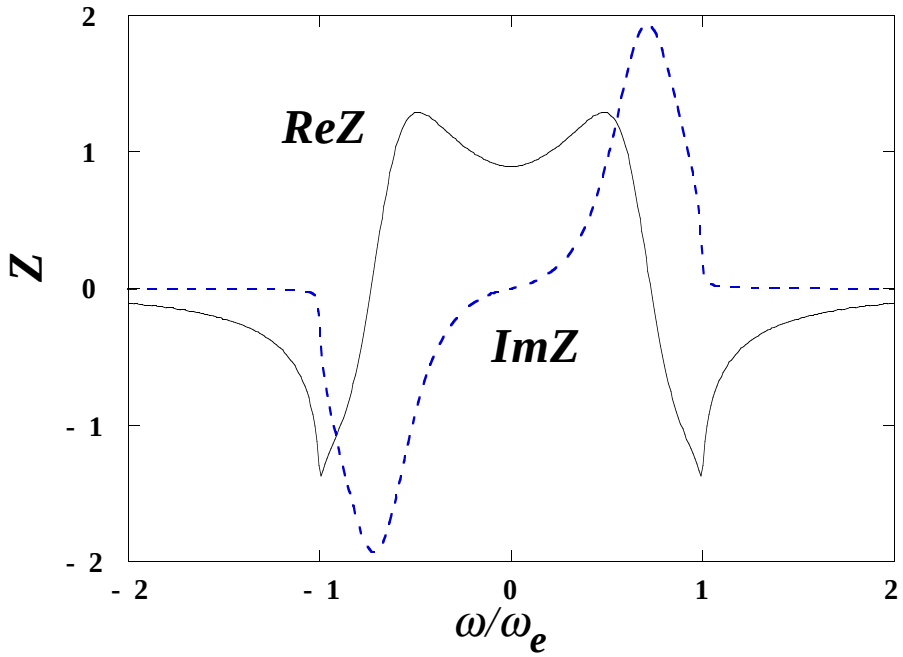

FIG. 4

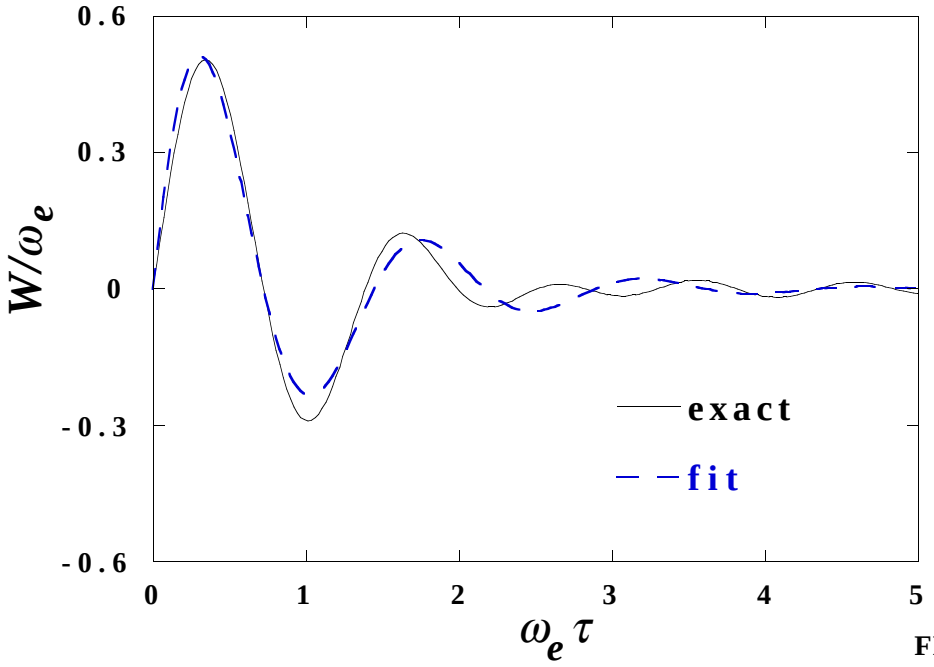
0.6
0.3
0
-0.3
-0.6
W/ω_e
0
1
2
3
4
5
ω_e τ
exact
fit

FIG. 5

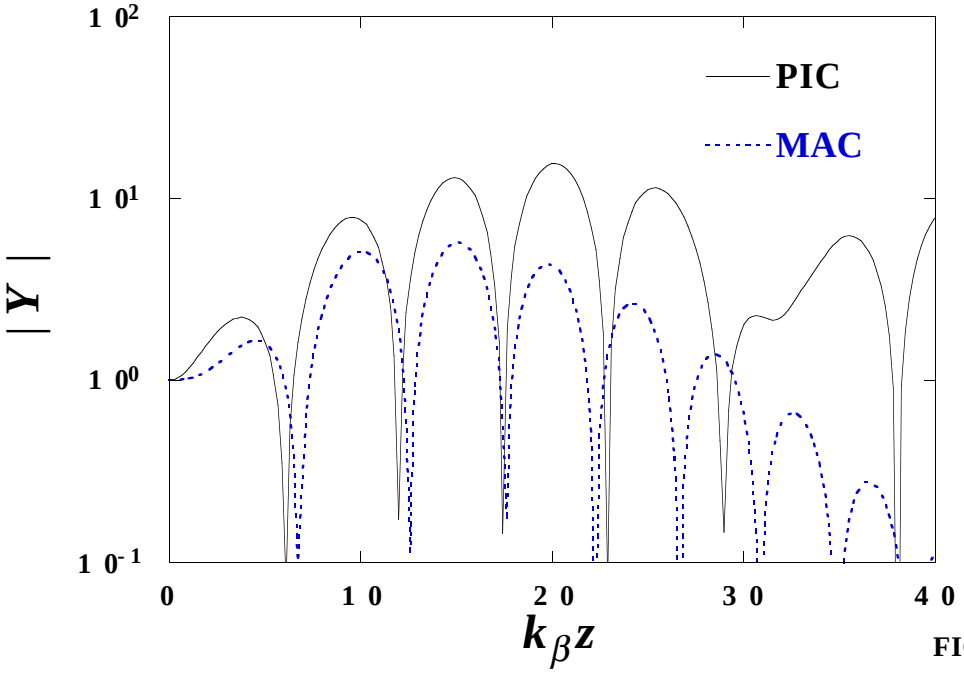
10^2
10^1
10^0
10^-1
|Y|
0
10
20
30
40
k_β z
PIC
MAC

FIG. 6

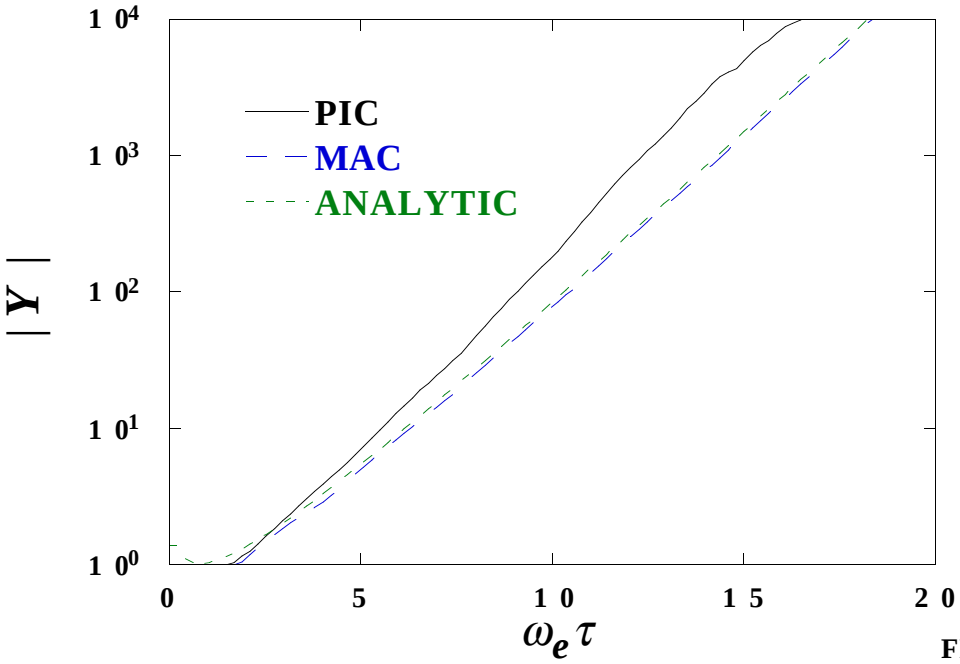

FIG. 7